

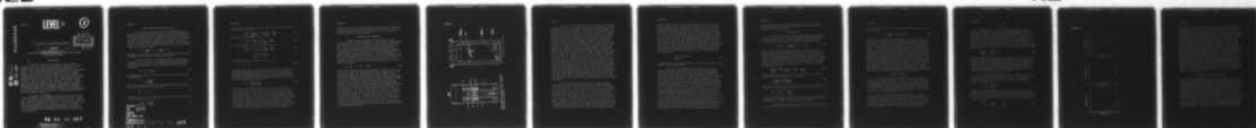
AD-A056 445 ARMY MOBILITY EQUIPMENT RESEARCH AND DEVELOPMENT COMM--ETC F/G 19/1
HARDENING OF COUNTERMINE STRUCTURES, (U)
JUN 78 D C HEBERLEIN

UNCLASSIFIED

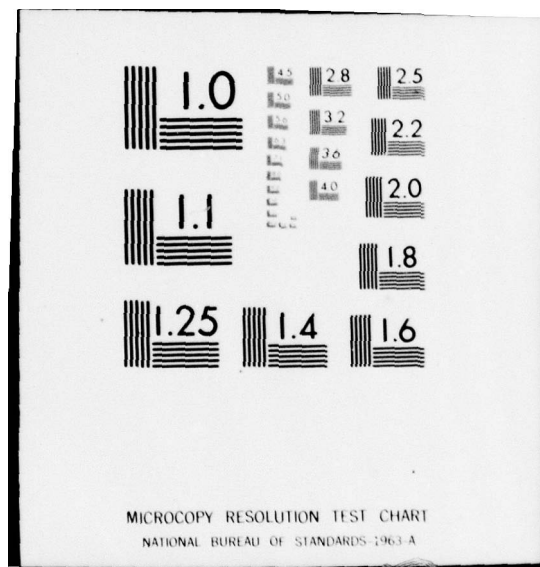
NL

1 of 1

AD
A056 445



END
DATE
FILMED
8 -78
DDC



AD A 056445

HEBERLEIN

LEVEL II



DDC
RECEIVED
JUL 12 1978
D

6 HARDENING OF COUNTERMINE STRUCTURES

11 JUN 1978

12 15p

10 DAVID C. HEBERLEIN PhD

US ARMY MOBILITY EQUIPMENT RESEARCH AND DEVELOPMENT COMMAND
FORT BELVOIR, VIRGINIA

INTRODUCTION

Mines have long been recognized and used as effective barriers to retard or restrict the advance of enemy forces. Mines contain a sensor for target acquisition and an explosive kill mechanism that is directed towards a vulnerable area of an acceptable target. Mine explosive kill mechanisms include blast damage to armored vehicle tracks, wheels and suspension systems, shrapnel damage to personnel or non-armored vehicles, and shape charge damage to the "belly" of armored vehicles. Mine terminal effects can be defeated through the use of high strength, light weight composite materials. Vehicle components and countermine structures can be made from composite materials that will retain their functionality after being exposed to blast loading or high velocity fragments. Although these components are damaged by the mine, the retention of functionality permits the completion of mission. It is in this sense that vehicles and countermine structures are hardened against mine blast and shrapnel damage.

Computer codes are being developed to evaluate mine blast and shrapnel damage to countermine structures and vehicles. These codes are presently predicting damage to traditional armor steels for which a wealth of experimental data exists. The composite literature, while rapidly expanding, is not adequate to establish the shock compression equations-of-state for these materials. The objective of this investigation is to provide an experimental base for constructing the shock compression equations-of-state for selected composite materials.

78 06 12 037

DISTRIBUTION STATEMENT A
Approved for public release;
Distribution Unlimited

403 160

JOB

AD No.
DDC FILE COPY

HEBERLEIN

SHOCK COMPRESSION EQUATION-OF-STATE

The utility of computer codes to meaningfully predict structural response to shock deposition is largely determined by the accuracy and completeness of the data used to determine the shock compression equations-of-state. Because structures are both heated and compressed during shock loading it is necessary to determine the temperature dependence of all independent variables in order to predict the time dependent response of the structure. The approach chosen to determine the material coefficients, A and B, in the shock compression equation-of-state

$$P = A (\rho/\rho_0 - 1) + B (\rho/\rho_0 - 1)^2, \quad (1)$$

where ρ is the material mass density, also determines whether $A=A(T)$ and $B=B(T)$ can be obtained from experimental data.

One direct method to obtain the temperature dependence of the material coefficients is through the Gruneisen formulation of the Debye theory of solids. An approach suggested by Harris and Avrami¹ expands Equation 1 above in terms of V for small volume changes as:

$$PV = A' V_0 + B' \frac{V_0}{V} + C'. \quad (2)$$

The Gruneisen parameter, Γ , can be expressed in terms of the speed of sound, c_0 , as

$$\Gamma = - \frac{v}{c_0} \left(\frac{\partial c_0}{\partial v} \right)_T \quad (3)$$

where c_0 is defined in terms of the longitudinal sound velocity, c_1 , and the transverse sound velocity, c_t , as

$$\frac{1}{c_0^3} = \frac{1}{c_1^3} + \frac{2}{c_t^3} \quad (4)$$

Equations 2 and 3 can be combined to give the speed of sound in terms of the shock pressure, P, to give

$$c_0(\rho) = \left(\frac{\partial P}{\partial \rho} \right)^{1/3} \quad (5)$$

ACCESSION by	
DTIC	White Section <input checked="" type="checkbox"/>
DDP	Buff. Section <input type="checkbox"/>
UNANNOUNCED	<input type="checkbox"/>
JUSTIFICATION	
Per Basic rpt.	
BY _____	
DISTRIBUTION/AVAILABILITY CODES	
Dist. AVAIL. and/or SPECIAL	
A	

78 06 12 037

HEBERLEIN

From equation 5, the speed of sound can be expressed in terms of the material coefficients by

$$c_o (f) = \left(\frac{A}{f_o}\right)^{1/2} \left(1 + \frac{2B}{A} \left(\frac{f}{f_o} - 1\right)\right)^{1/2}, \quad (6)$$

which can be approximated to give:

$$c_o (f) \approx c_o \left\{1 + \frac{B}{A} \left(\frac{f}{f_o} - 1\right)\right\}. \quad (7)$$

For $(B/A) \left(\frac{f}{f_o} - 1\right) \ll 1$, equation 7 reduces to

$$\frac{v}{c} \frac{\partial c_o}{\partial v_o} \approx \frac{v}{c} \frac{\partial}{\partial v} \left\{ c_o \frac{B}{A} \left(\frac{v_o}{v} - 1\right) \right\} \quad (8)$$

$$= - \frac{v}{c} \left\{ c_o \frac{B}{A} \frac{v_o}{v^2} \right\}, \quad (9)$$

giving the Gruneisen parameter at $v = v_o$ as

$$\Gamma = \frac{B}{A}. \quad (10)$$

The importance of this result is that the material coefficients for the shock compression equation-of-state can be established from fundamental thermodynamic properties of the materials themselves. The temperature dependence of the Gruneisen parameter is given by the thermal expansion coefficient, α , the specific heat, C_v , and the isothermal compressibility, K_T , as

$$\Gamma(T) = \frac{\alpha(T) v(T)}{C_v(T) K_T(T)}. \quad (11)$$

Thus, the temperature dependence of the ratio of the material coefficients of the shock compression equation-of-state may be determined directly through measurements of the thermal expansion coefficient, specific heat and isothermal compressibility. This paper reports experimental data of relative volume changes, thermal expansion coefficient, and specific heat as functions of temperature for selected composite materials over the temperature interval 240 to 370 K. These data when combined with sound velocity data are used to construct the time dependent shock compression equation-of-state for each material. The formulation of the computer code requires that three independent equations for shock pressure,

HEBERLEIN

changes in internal energy, and the elastic pressure are expressed in terms of the material coefficients and the material mass density such that specification of initial conditions and the shock conditions defines the shock deposition process.

APPARATUS AND TECHNIQUES

The apparatus for measuring the length changes in the composite samples is shown in Figure 1. The changes in sample length were observed as changes in capacitance. The capacitor was of the three-terminal type. The area of the fixed, guarded plate was 6.41 cm². The capacitor gap was nominally 0.020 cm, resulting in a capacitance of approximately 20 pF. The capacitance was measured to approximately 1 part in 10⁵, giving a length resolution of 10⁻⁷cm. Sample lengths were typically 0.254 cm. A calibrated platinum resistance-thermometer was situated in a well in the sample platform. The stated calibration was checked both at the ice point and against the vapor pressure of liquid nitrogen between 64 and 77 K. The calibration points for the resistance R and temperature T were used in the relationship,

$$R = R_0 (1 + \xi T + \eta T^2), \quad (12)$$

to determine values for the constants ξ and η . Values for these constants were found that represented the stated calibration to an rms deviation of 0.03K over the temperature interval 230 to 370 K. Temperature changes were detected as resistance changes using a Hewlett Packard 3490A Multimeter. This instrument uses a four terminal measurement technique detecting changes as small as 0.001 ohm. The stated accuracy of the resistance measurement is 0.0001 percent. During the course of the experiments, the Hewlett Packard 3490A Multimeter and the Hewlett Packard 4270A Automatic Capacitance Bridge were used in the remote, addressed mode for acquiring data and transmitting it to a Hewlett Packard 9830A Calculator for data storage and display. The sample chamber was surrounded by a can into which helium exchange gas was introduced. A vacuum space thermally isolated this can from a surrounding liquid bath. A heater was wound on the exchange gas can to maintain the entire sample chamber assembly shown in Figure 1 at the desired temperature. The data acquisition system was programmed to maintain each temperature for a total of thirty measurements at each temperature. The capacitance-temperature data were then averaged before being stored in the memory of the HP 9830A Calculator.

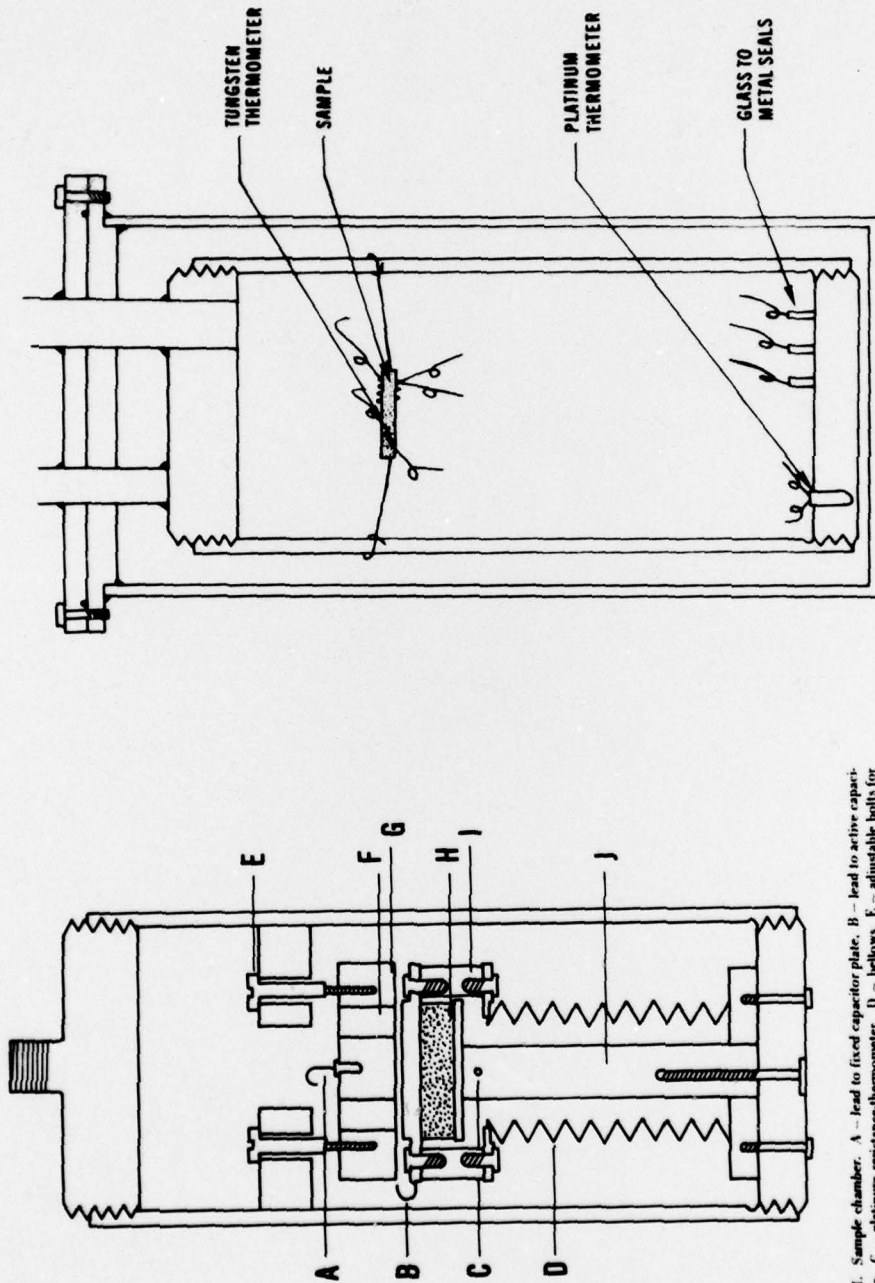


Figure 1. Sample chamber. A - lead to fixed capacitor plate, B - lead to active capacitor plate, C - platinum resistance-thermometer, D - bellows, E - adjustable bolts for fixed capacitor plate, F - concentric secondary capacitor plate, G - guard ring, H - sample, I - nylon posts, J - sample platform.

Figure 2. Sample chamber for heat capacity measurements.

HEBERLEIN

The sample chamber used for the heat capacity measurements is shown in Figure 2. The sample chamber was surrounded by a vacuum can which was used as an adiabatic heat shield about the sample during the heat pulse measurements. A 100-ohm heater was wound on the outside of this inner vacuum can. The inner vacuum can was thermally isolated from the bath temperature by an outer vacuum can. During temperature calibration, the inner vacuum chamber was filled with helium exchange gas. This insured that the sample temperature was the same as that of the sample chamber assembly. The composite samples were suspended by two 0.002 cm diameter nylon wires from the walls of the sample chamber. The thermometer and heater leads to the sample were thermally anchored to glass-to-metal seals, which were soldered into the base of the copper sample chamber. Copper wires, 0.002 cm in diameter, were used as leads from the glass-to-metal seals to the sample to minimize the heat leak from the sample chamber to the sample. The sample heater was a 0.004 cm diameter constantin wire noninductively wound on the outside of the sample. A four terminal circuit was used to measure the current and voltage across the sample heater. The sample heater current was measured in terms of the voltage drop across a 1-kilohm resistor maintained in an external oil bath. The voltage across the 1-kilohm resistor and the voltage across the heater were measured with a Hewlett Packard 3490A Multimeter. The time duration of the heat pulse was detected with a Hewlett-Packard 5328A Frequency Counter. The stated accuracy of these measurements was better than 0.001 percent for the ranges which were used. The primary thermometer used in these measurements was a calibrated platinum resistance-thermometer as described for the relative length change measurements. The platinum resistance thermometer was situated in a well in the base of the sample platform shown in Figure 2.

Because the size of the samples was generally small (typically less than 3 grams), the mass of the sample thermometer was a major factor in maintaining the absolute accuracy of the heat capacity measurements. The use of standard resistance thermometry was precluded by the size and weight of commercially available platinum, germanium, and carbon resistors. The choice of the sample thermometer was also based on the nominal resistance of the temperature sensor, its temperature sensitivity, and its reproducibility on thermal cycling. The sample thermometer chosen consisted of a 5 cm piece of 0.0004 cm tungsten wire wound non-inductively about the sample. The wire was obtained in the form of a 100 ft (30.3 m) spool from Sigman Cohn Corporation. The tungsten wire was attached to the composite samples using a fine resin spray. This method of attachment proved to provide good thermal contact between the thermometer

HEBERLIEN

and the sample. The room temperature resistance of the tungsten resistance-thermometer was typically 100 ohms. The total resistance of the tungsten resistance thermometer changed by a factor of 1.64 between 240 and 370 K. Changes in the resistance of the tungsten resistance-thermometer were detected using a Hewlett Packard 3490A Multimeter. The 3490A Multimeter uses a bridge principle for measurement such that the nominal heat supplied to the temperature sensor was less than 1 picowatt. In order to maintain a high precision of temperature accuracy for the small temperature excursions of the sample during and after the application of the heat pulse, a function was determined that gave the tungsten wire resistance in terms of the temperature. The fit of the tungsten resistance over the temperature interval 240 to 370 K had an rms deviation equal to or better than that for the primary platinum thermometer. The function used to determine the temperature from the resistance of the tungsten wire was of the form:

$$T = \sum_{i=0}^{i=4} A_i R \quad (\text{slope})^i \quad (13)$$

Using this function, the 9830A Calculator could quickly and accurately calculate sample temperatures.

The inner vacuum chamber was evacuated during the heat pulse measurements. The inner vacuum can and the copper sample chamber were maintained at a constant temperature during the heat pulse measurements and, thereby, served as adiabatic heat shields. The temperature of the adiabatic shield and the sample were maintained at the same temperature for a period of 60 seconds before a heat pulse sequence was initiated. After equilibrium between the sample temperature and the sample chamber assembly had been maintained for a period of 60 seconds, the sample temperature was allowed to drift cold for a period of 30 seconds. This temperature drift before and after the application of the heat pulse was used to correct for the true temperature excursion during the application of a heat pulse. The heat pulse duration was typically 15 seconds during which time a Hewlett Packard 3490A Multimeter was used to make at least 15 separate readings of heater voltage, heater current and sample temperature. After 15 seconds, the current to the heater was shut off automatically and the temperature of the sample recorded as a function of time for 200 seconds. The change in sample temperature was determined by extrapolating the temperature drift both before and after application of heat to the center of the heat pulse. The entire process was controlled by a program entered into the memory of the 9830A Calculator. All data collection and analyses were performed

HEBERLEIN

entirely within the Hewlett Packard 3050B Data Acquisition System. A permanent record of each heat pulse was recorded with a Hewlett Packard 9862A Thermal Printer.

DATA ANALYSIS

The raw data for the relative length change measurements consisted of a series of values of capacitance versus temperature at essentially zero pressure. The capacitance C for a three-terminal capacitor using a guard ring is related to the gap length l_g by

$$C = \frac{\pi \epsilon r^2}{l_g} + \frac{\pi \epsilon r w}{l_g + 0.22w} \left(1 + \frac{w}{2r} \right) \quad (14)$$

where r is the radius of the plate with the guard ring, ϵ is the permittivity, and w the half-width of the spacing between the inside radius of the guard ring and the radius of the plate. The experimental geometry $r \gg w$ made the effect of the last term in Equation 14 on dC/C less than 0.3 percent and was neglected. Changes in sample length l_s are found directly in terms of C from Equation 14 because $l_s + l_g = \text{constant}$. The linear expansion coefficient was obtained by differentiating Equation 14 with respect to temperature at constant pressure to give:

$$\left(\frac{dl_g}{dT} \right)_p = \frac{\pi \epsilon r^2}{C^2} \left(\frac{dC}{dT} \right)_p + \frac{2\pi \epsilon r}{C} \left(\frac{dr}{dT} \right)_p \quad (15)$$

The last term in Equation 15 was also neglected because the radial expansion of the copper plates was small; i.e.

$$\frac{1}{C} \left(\frac{dC}{dT} \right)_p \gg 10^4 \left(\frac{1}{r} \right) \left(\frac{dr}{dT} \right)_p \quad (16)$$

Since the gap length change is equal and opposite to the sample length change, $dl_s = -dl_g$, the linear expansion coefficient is given by

$$\alpha_l = \frac{\pi \epsilon r^2}{l_s C^2} \left(\frac{dC}{dT} \right)_p \quad (17)$$

Because measurements were taken along three perpendicular axes for each sample, the volume expansion coefficient was obtained by adding the three linear expansion coefficients for each sample.

The specific heat of a material is defined as the heat capacity normalized per mass, volume, or mole. For a solid maintained

HEBERLEIN

at essentially zero pressure, the specific heat at constant pressure, C_p is given by:

$$C_p = \frac{1}{m} \frac{(\Delta Q)}{(\Delta T)} = \frac{1}{m} \frac{V_h I_h \delta t}{T} \quad (18)$$

where m is the mass of the sample, ΔQ the total amount of heat added to the sample, V_h , the voltage across the heater, I_h , the current in the heater, and δt the total time the heater was on. The heat leak from the heater leads to the sample was corrected through the use of a three-terminal measurement technique of heat supplied to the heater. In this technique two matched leads are connected from the glass-to-metal seals in the base of the chamber assembly to one side of the sample heater. A third matched lead extends from the other side of the sample heater to a third glass-to-metal seal thermally anchored to the sample platform assembly. In this manner, exactly one-half of the ohmic heating occurring in these lead wires is automatically counted in the measurement of power supplied to the sample heater. The other half of the ohmic heating is not counted because it is absorbed by the sample platform assembly. The additional heat capacity of the sample heater and thermometer was much smaller than that of the composite samples, $C_{\text{sample}} \geq 10^2 (C_{\text{htr}} + C_{\text{therm}})$, and corrections to the calculated specific heat values for the masses of the heater and sample thermometer were also neglected.

COMPOSITE SAMPLES

The composite samples were obtained from Dr. I. Daniel, IIT Research Institute, Chicago, Illinois. The samples selected were representative of different types of composites as well as similar materials with different plies. The composite selection included cross-ply E-Glass, cross-ply S-Glass, unidirectional S-Glass, boron/aluminum 1928-9, boron/aluminum 1928-11 and KEVLAR. The c -axis was taken as that axis perpendicular to the plies. The a and b axes were identified as spatially orthogonal to the c axis.

The resin composites absorb moisture from the air over prolonged periods of exposure. Before the samples were mounted in the sample chamber, each sample was held in an oven at 373 K for a period of approximately 1 week. After the samples were mounted in the sample chamber, the samples were heated to 380 K, and a vacuum established about the sample. The heated samples were maintained in vacuo for a period of day before experiments were initiated.

RESULTS

A typical plot of relative length change versus temperature is shown in Figure 3 for the \underline{c} -axis of a KEVLAR/ERLA 4617 sample. The linear expansion coefficient can be obtained through a point-by-point differentiation of the data shown in Figure 3. The scatter inherent in this technique is approximately $\pm 5\%$. In order to handle the numerous calculations for which these data will be used, a different technique was used to calculate the linear expansion coefficient. An analytic function was calculated to fit the relative changes in length. Typically, 8 to 10 points from the relative length change versus temperature curves were used to find an analytic function of the form:

$$\frac{\Delta \ell_s(T)}{\ell_s(T)} = \sum_{i=0}^{i=N} A_i T^i \quad (19)$$

The linear expansion coefficient is then found by differentiating the analytic function found from Equation 19 with respect to temperature. The linear expansion coefficient corresponding to the data shown in Figure 3 for relative length changes along the \underline{c} -axis in KEVLAR is shown in Figure 4. The volumetric expansion coefficient is then obtained by adding the linear expansion coefficients for the three independent spatial axes. The volumetric expansion found for samples of boron/aluminum 1928-9 is shown in Figure 5.

The specific heat data were taken at approximately 0.5 K temperature increments from 240 to 370 K. The raw specific heat data for cross-ply S-Glass epoxy composite is shown as a function of temperature in Figure 6. To facilitate handling of the data, an analytic function of the form

$$C_p(T) = \sum_{i=0}^{i=9} C_i T^i \quad (20)$$

was fit to ten experimental specific heat versus temperature data points. From the smoothed curves obtained for the volumetric expansion coefficient and those obtained for the specific heat from Equation 20, it is possible to show the temperature dependence of Γ/C_0^2 , where C_0 is the speed of sound in the solid material. The Gruneisen parameter is given by

$$\Gamma(T) = \frac{\alpha V}{K_T C_V} = \frac{\alpha C_0^2}{C_V} \quad (21)$$

HEBERLEIN

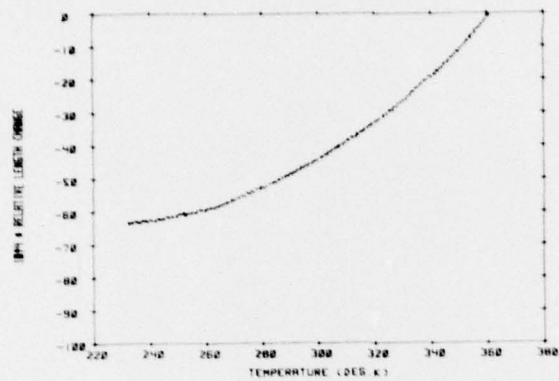


Figure 3. Relative Length Change of ANTLAR POLA 4077 (Gardex)

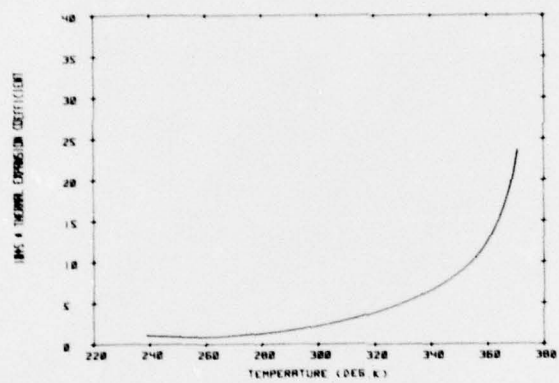


Figure 4. Linear Expansion Coefficient for ANTLAR POLA 4077 (Gardex)

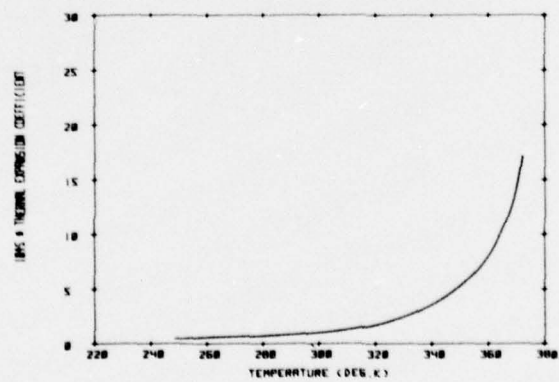


Figure 5. Volumetric Expansion of Borethiastudium 1828-11

HEBERLEIN

The temperature dependence of the quantity $10^{11} \rho/C_0^2$ (g/erg) is shown for samples of cross-ply E-Glass and cross-ply S-Glass epoxy composites in Figures 7 and 8 respectively. Because the experimental data that leads to the formation of Figures 7 and 8 is too voluminous to present herein, the differences in their temperature dependence is summarized. The heat capacities of the S-Glass composites were found to be higher than those measured for the E-Glass composites. The thermal expansion coefficients, while the same order of magnitude for both type of Glass epoxy composites, exhibited a much stronger temperature dependence for the S-Glass composites. In fact, both S-Glass composites exhibited a negative volumetric expansion coefficient for temperatures below approximately 325 K. Because the isothermal compressibility is generally slowly varying with temperature over the temperature interval of interest, it can be seen from Equation 21 that the quantity α/C_v shown in Figures 7 and 8 is a good approximation to the temperature dependence of the Gruneisen parameter. Although neither isothermal compressibility nor sound velocity measurements are presently available over this temperature interval, it is reasonable to assume that the strong temperature dependence of α/C_v shown in Figures 7 and 8 and similarly found for the other composites measured in this investigation indicates that the use of only the room temperature value of the Gruneisen parameter in shock compression equations-of-state will lead to erroneous or uninterpretable predictions of the time dependent response of a composite material to shock loading.

APPLICATIONS TO DEVELOPMENTAL WORK

Composite materials present certain physical properties that make them promising candidates for use in hardening vehicles and countermine equipment to mine blast and shrapnel damage. The heat capacities measured for the composite materials are of the same order of magnitude as that found for strong metals. The composite materials are capable of absorbing large quantities of energy from shock loading. The thermal expansion of composite materials is generally slightly higher than that used in armor materials. The composite materials are considerably lighter than armor materials while retaining strength properties equal to that found in armor steels. The composites can be formed with the reinforcement plies perpendicular to the direction of anticipated loading. Armor steels are essentially homogeneous solids and critical loading results in catastrophic failure to an entire structure. Composite materials, while exhibiting local failure to blast loading, retain their structural form and thus their functionality. In addition, the composite material absorbs

HEBERLEIN

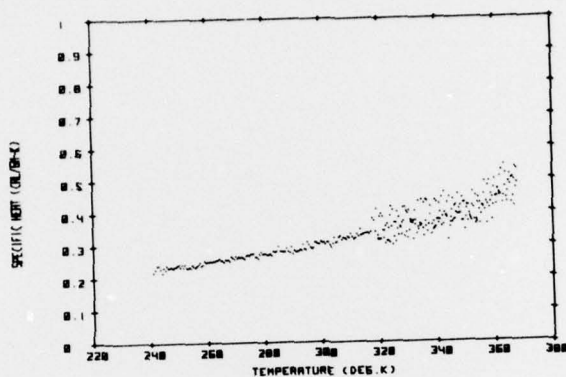


Figure 6. Specific heat of cross-ph. A Glass epoxy.

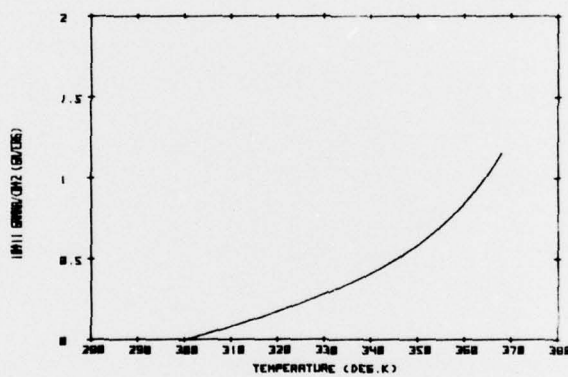


Figure 7. Gruneisen parameter for cross-ph. F Glass epoxy.

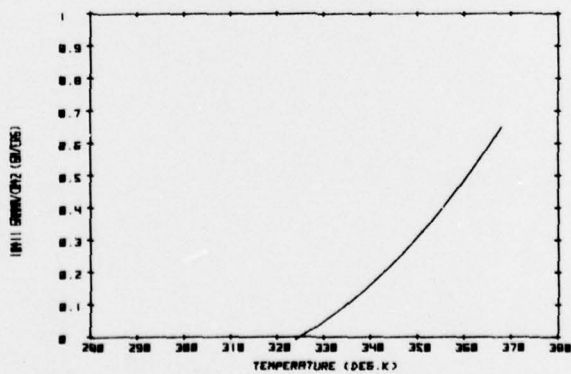


Figure 8. Gruneisen parameter for cross-ph. S Glass epoxy.

HEBERLEIN

large amounts of the shock energy and does not pass this energy through it to some other weaker link in the structure.

For development work, it is necessary to consider not only the physical properties of the composite materials but also the cost of acquisition and tooling workable structures. Shown in Figure 9 is a cylindrical form built principally of low cost KEVLAR. This particular KEVLAR structure has been subjected to the blast and shrapnel from ten M-21 mines (M-21 mines contain 10 lb of H-6 explosive). The structure survived these repeated shots at distances ranging from 2 to 6 feet at the solid angle found to have the highest density of metal mine fragments. This particular structure was developed to protect a countermine coil, used to clear magnetic influence mines, from blast and shrapnel damage. Shown in Figure 10 are two fully hardened countermine coils to be used in field testing against live mines. The composite material used to harden the coil to blast and fragment damage amounts to less than 40% of the weight of the total coil structure.

CONCLUSIONS

Future measurements of the sound velocity of these composites will define the temperature dependence of the Gruneisen parameter and the temperature dependence of the ratio of the material coefficients in the shock compression equations-of-state. These data will permit the development of predictive codes that can trace the time evolution of shock deposition in various structures. The high specific heat values found for composites indicates that these materials can be used to absorb large quantities of energy and thereby preclude the passage of this energy to weaker links in the structure. The temperature dependence of the quantity α/C_v indicates a strong dependence of the Gruneisen parameter, Γ , on temperature and consequently the importance of defining $B(T)/A(T)$ for composites before development of predictive codes.

REFERENCES:

P. Harris and L. Avrami, "Some Physics of the Gruneisen Parameter", Picatinny Arsenal Technical Report No. 4423, September 1972.

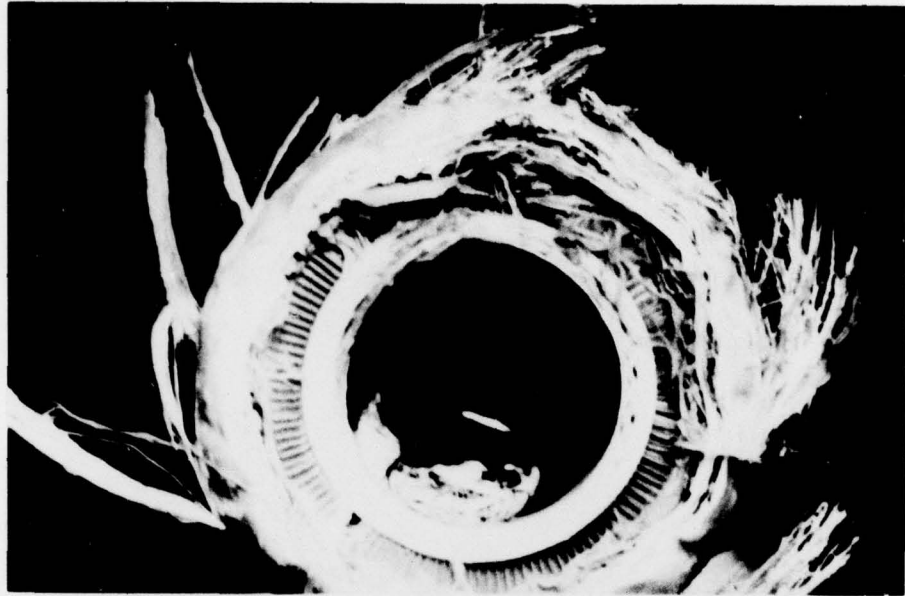


Fig. 9. Countermine Coil Form Subjected to Repeated Blast and Shrapnel of M-21 Mines

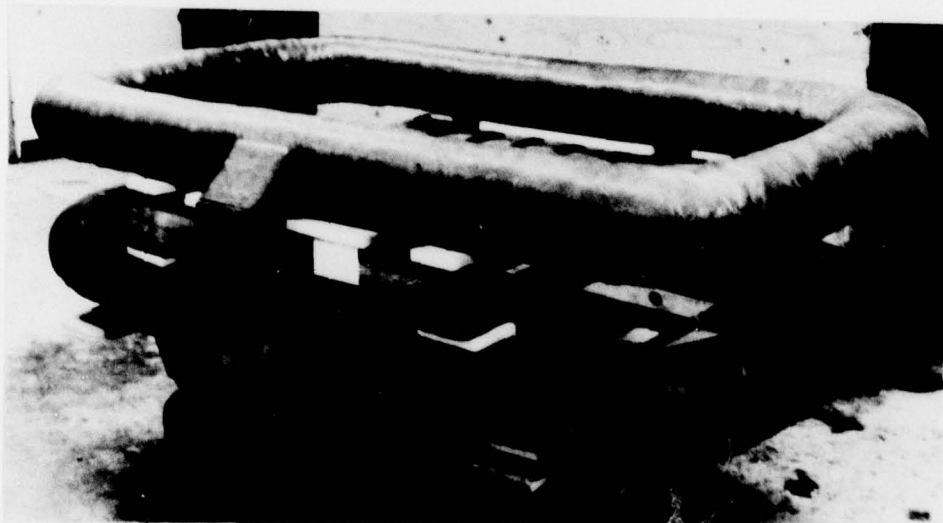


Fig. 10. Two Completely Hardened Countermine Coil Forms